EFFECT OF ION CONCENTRATION CHANGES IN T-TUBULES ON INTRACELLULAR SIGNALS CONTROLLING MECHANICAL ACTIVITY IN A MODEL OF HUMAN VENTRICULAR CARDIOMYOCYTE

Dana Hrabcová*, Michal Pásek*,**, Jiří Šimurda*, Georges Christé***

The transverse (t-) tubular system serves to bring electrical signals deep inside the muscle cells to control mechanical responses. Our preliminary mathematical model of human ventricular cardiomyocyte incorporating t-tubular system [1] was improved by introducing description of latest experimental data related to morphology of human t-tubules and to specific properties of ionic currents. To describe the ion diffusion within t-tubular lumen, we partitioned the t-tubule compartment into nine concentric cylindrical segments. Using the model, we studied the effect of activity-induced concentration changes in the t-tubules on Ca^{2+} entry into the cell and the intracellular Ca^{2+} transients controlling the strength of cellular contraction. The values of some crucial parameters, unknown in human cardiomyocytes to date, were regarded as independent variables. The simulations confirmed the tendency of the activity-induced t-tubular concentration changes of Ca^{2+} to reduce the Ca^{2+} entry into the cell as well as the intracellular Ca^{2+} transient. The effect rose with the increase of t-tubular fraction of L-type Ca^{2+} channels ($f_{\mathrm{Ca,t}}$), with the decrease of t-tubular fraction of Ca^{2+} pump ($f_{\mathrm{pCa,t}}$) and with the increase of the time constant of Ca^{2+} exchange between external space and t-tubule lumen ($\tau_{\mathrm{Ca,extt}}$). Significant effect occurred if simultaneously $f_{\mathrm{Ca,t}} \geq 0.64$, $f_{\mathrm{pCa,t}} \leq 0.2$, and $\tau_{\mathrm{Ca,extt}} \geq 240\,ms$.

Keywords: *human heart, cardiac cell, t-tubule, quantitative modeling*

1. Introduction

In our previous work, we developed a mathematical model of human ventricular cell electrical activity that was the first to include a quantitative description of the transverse (t-) tubular system [1]. The preliminary simulations indicated that the electrical activity induces significant transient changes of Ca^{2+} and K^+ concentration in human t-tubules that may reduce intracellular Ca^{2+} load and cytosolic Ca^{2+} transient controlling mechanical activity. A similar effect was observed in our previously published animal models [2], [3].

In this paper, we describe a more elaborate version of the model that is based on recently published data from human cardiomyocytes regarding the detailed morphology of the t-tubules and the particular properties of ion transfer mechanisms. In addition, we refined the description of the t-tubular lumen by considering several concentric layers with the aim

* Mgr. D. Hrabcová, doc. Ing. M. Pásek, Ph.D., doc. RNDr. Ing. J. Šimurda, CSc., Department of Physiology, Masaryk University, Brno, Czech Republic

** doc. Ing. M. Pásek, Ph.D., Institute of Thermomechanics – Branch Brno, Czech Academy of Science, Brno, Czech Republic

*** G. Christé, PhD, EA4612, Neurocardiology, University Claude Bernard Lyon1, Lyon, France

to simulate more precisely the ion diffusion within the t-tubules and between the t-tubular and external space. The model is aimed to provide an insight into the extent of dynamic changes in ion concentrations near the human t-tubular membrane and into their effect on the quantities that play an important role in excitation-contraction coupling.

2. Modification of the Model

2.1. Model structure

The model is based on the latest quantitative description of guinea pig ventricular cell electrical activity [3]. It was modified (for structure of the model see Fig. 1) to respect the recently published data related to morphology of human ventricular cardiomyocytes and to properties of ion transfer mechanisms.

We assumed a cell with capacitance of cellular membrane of 107 pF. The total membrane area computed from the commonly used membrane specific capacitance $1\,\mu\mathrm{F/cm^2}$ was $10700\,\mu\mathrm{m}^2$. To keep all geometric parameters of the model cell consistent with surface/volume ratios ($A_{\mathrm{tot}}/V_{\mathrm{cell}} = 0.729\,\mu\mathrm{m}^2/\mu\mathrm{m}^3$, $A_{\mathrm{tub}}/V_{\mathrm{cell}} = 0.403\,\mu\mathrm{m}^2/\mu\mathrm{m}^3$, $A_{\mathrm{tub}}/V_{\mathrm{cell}} = 0.327\,\mu\mathrm{m}^2/\mu\mathrm{m}^3$), fractional area of t-tubular membrane (0.56) and mean radius of the t-tubules (210 nm) published by Ohler et al. [4], the fractional volume of t-tubular system must have been reduced from 0.0867 [4] to 0.042. The resulting volume of the model cell was than 14.9 pL. The fractional volumes of intracellular compartments (myoplasm 0.68, NSR 0.055, JSR 0.0042 and dyadic space 0.00002) were adjusted to be consistent with the model of human ventricular myocyte published by Iyer et al. [5].

To simulate the ion gradient in the t-tubular lumen, the system (each t-tubule) was partitioned into 9 concentric cylindrical segments S_{t1}, S_{t2}, . . . , S_{t9} (Fig. 1 – bottom part). To increase the accuracy of computation of ion concentration changes in the vicinity of t-tubular membrane, the volumes of segments $S_{\mathrm{t1}} - S_{\mathrm{t8}}$ were set to 3 % of the total t-tubular volume; further reduction of the segments or increase of their number did not significantly alter the results.

2.2. Membrane transport system

The description of membrane currents was modified to be consistent with recently published models of human cardiomyocytes. The formulations of I_{Na}, I_{Ca} and I_{K1} were adopted from [5] and those of I_{Kr}, I_{Ks} and I_{Kto} from [6]. The less important currents I_{Kp} and $I_{\mathrm{K(ATP)}}$ were omitted.

To obtain an acceptable fit of the model results with experimental data from [7] the steady-state voltage dependent inactivation of I_{Ca} (y_∞) and the time constant of I_{Kto}-inactivation (τ_{s}) were reformulated. Their final forms are:

$$y_\infty = \frac{0.82}{1 + \mathrm{e}^{(V_{\mathrm{m}}+28.5)/7.8}} + 0.1\ , \tag{1}$$

$$\tau_{\mathrm{s}} = 0.085\,\mathrm{e}^{-(V_{\mathrm{m}}+45)^2/320} + \frac{0.005}{1 + \mathrm{e}^{(V_{\mathrm{m}}-63)/5}} + 0.003\ . \tag{2}$$

The maximum conductivities, currents or permeabilities of ion transporting systems (Tab. 1) were set for the model to generate physiological levels of intracellular ion concentrations as well as configurations of action potentials in the whole range of stimulation

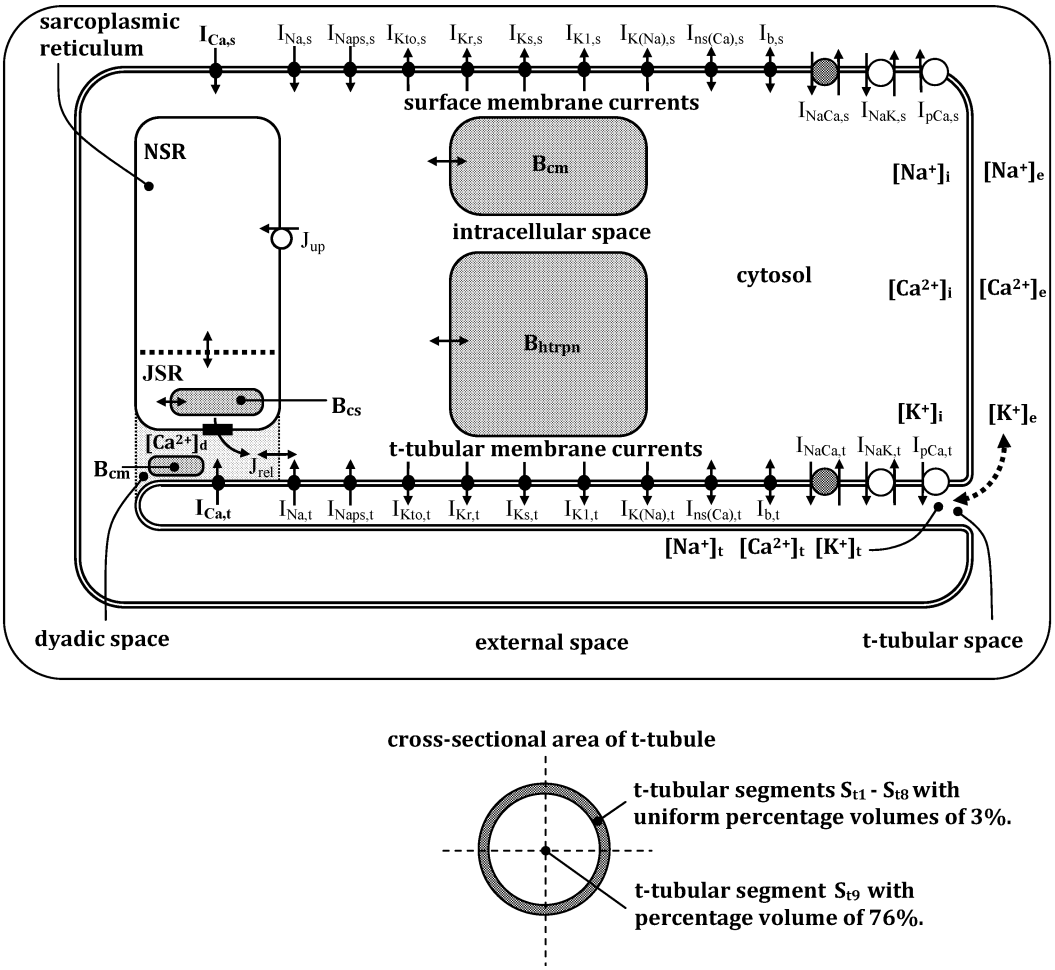

Fig.1: Schematic diagram of the human ventricular cell model used in the present study. The description of the electrical activity of surface (s) and t-tubular (t) membranes comprises formulations of the following ion currents: fast sodium current (I_{Na}), persistent sodium current (I_{Naps}), L-type calcium current (I_{Ca}), transient outward potassium current (I_{Kto}), rapid and slow components of delayed rectifier potassium current (I_{Krs} and I_{Krs}), inward rectifying potassium current (I_{K1}), background currents (I_b), sodium-activated potassium current ($I_{K(Na)}$), calcium-activated non-specific current ($I_{ns(Ca)}$), sodium-calcium exchange current (I_{NaCa}), sodium-potassium pump current (I_{NaK}) and calcium pump current (I_{pCa}). The intracellular space contains the cytosolic space (c), dyadic space (d), network and junctional compartment of sarcoplasmic reticulum (NSR, JSR), endogenous Ca^{2+} buffers (calmodulin (B_{cm}), troponin (B_{htrpn}, B_{ltrpn}) and calsequestrin (B_{cs}). The t-tubular space is partitioned into nine concentric segments, $S_{t1} - S_{t9}$; a schematic representation of this partitioning is shown under the diagram. J_{up} represents Ca^{2+} flow via SR Ca^{2+} pump and the small filled rectangle in JSR membrane ryanodine receptors. The small bi-directional arrows denote Ca^{2+} diffusion. Ion diffusion between the tubular and external space is represented by the dashed arrow.

frequencies characteristic for the human heart [7], [8], [9]. The distribution of ion transporters between the surface membrane and the t-tubular membrane (Tab. 1) as well as the time constants controlling exchange of ions between external space and t-tubular lumen ($\tau_{\mathrm{Ca,extt}} = 240\,\mathrm{ms}$, $\tau_{\mathrm{K,extt}} = \tau_{\mathrm{Na,extt}} = 200\,\mathrm{ms}$) were set consistently as in guinea pig model [3] because of the paucity of experimental data from human cells.

$g_{\mathrm{Na,max}}$	$25\,\mathrm{mS\,cm^{-2}}$	$f_{\mathrm{Na,t}}$	0.57
$g_{\mathrm{Naps,max}}$	$0.01\,\mathrm{mS\,cm^{-2}}$	$f_{\mathrm{Naps,t}}$	0.56
P_{Ca}	$0.00185\,\mathrm{cm\,s^{-1}}$	$f_{\mathrm{Ca,t}}$	0.64
$g_{\mathrm{Kto,max}}$	$0.132\,\mathrm{mS\,cm^{-2}}$	$f_{\mathrm{Kto,t}}$	0.56
$g_{\mathrm{Kr,max}}$	$0.038\,\mathrm{mS\,cm^{-2}}$	$f_{\mathrm{Kr,t}}$	0.56
$g_{\mathrm{Ks,max}}$	$0.040\,\mathrm{mS\,cm^{-2}}$	$f_{\mathrm{Ks,t}}$	0.56
$g_{\mathrm{K1,max}}$	$0.125\,\mathrm{mS\,cm^{-2}}$	$f_{\mathrm{K1,t}}$	0.80
$g_{\mathrm{K(Na),max}}$	$0.129\,\mathrm{mS\,cm^{-2}}$	$f_{\mathrm{K(Na),t}}$	0.56
$g_{\mathrm{Nab,max}}$	$0.141\,\mu\mathrm{S\,cm^{-2}}$	$f_{\mathrm{Nab,t}}$	0.56
$g_{\mathrm{Cab,max}}$	$2.413\,\mu\mathrm{S\,cm^{-2}}$	$f_{\mathrm{Cab,t}}$	0.56
$P_{\mathrm{ns(Ca)}}$	$1.75\,\mathrm{nm\,s^{-1}}$	$f_{\mathrm{ns(Ca),t}}$	0.56
$k_{\mathrm{NaCa,max}}$	$0.15\,\mathrm{nA\,cm^{-2}\,mM^{-4}}$	$f_{\mathrm{NaCa,t}}$	0.56
$I_{\mathrm{NaK,max}}$	$0.975\,\mu\mathrm{A\,cm^{-2}}$	$f_{\mathrm{NaK,t}}$	0.56
$I_{\mathrm{pCa,max}}$	$1.725\,\mu\mathrm{A\,cm^{-2}}$	$f_{\mathrm{pCa,t}}$	0.20

Maximum conductivity ($g_{\mathrm{X,max}}$), current density ($I_{\mathrm{X,max}}$) or permeability (P_{x}) of ion transport systems used in the model. The values are related to the total membrane area. $f_{\mathrm{X,t}}$ represents the t-tubule fraction of the ion transporter underlying current I_{X}.

Tab.1: Electrical properties of ion transport systems in the model

2.3. Ion exchange between t-tubular segments and with the external space

The time constants controlling Ca^{2+} and K^+ exchange between the individual tubular segments were computed by multiplying the $\tau_{\mathrm{Ca,extt}}$ and $\tau_{\mathrm{K,extt}}$ by a factor taking into account the different diffusion area between individual segments and, in segments S_{t8} and S_{t9}, their different volumes. The resulting formulation is:

$$\tau_{\mathrm{X,St},n+1} = \tau_{\mathrm{X,extt}} \frac{A_{\mathrm{base},n}}{A_{\mathrm{boundary},n}} \frac{V_{\mathrm{St},n+1}}{V_{\mathrm{St},n}} , \tag{3}$$

where $\tau_{\mathrm{X,St},n+1}$ represent the time constant controlling the rate of diffusion of ion X from segment n to segment $n+1$ and the parameters $A_{\mathrm{base},n}$, $A_{\mathrm{boundary},n}$, $V_{\mathrm{St},n+1}$ and $V_{\mathrm{St},n}$ represent the area of segment n in the tubular mouth, area of the boundary between segments n and $n+1$, volume of segment $n+1$, and volume of segment n, respectively.

Because the concentration changes of tubular Na^+ are minimal, they are described in a single t-tubule compartment as in the guinea pig model [3].

2.4. Intracellular Ca^{2+}-handling

The formulation of intracellular Ca^{2+} handling is based on the description in the model of human ventricular myocyte published by Iyer et al. [5]. However, to prevent the intracellular Ca^{2+} overload and irregular Ca^{2+} release from JSR at higher stimulation rates a readjustment of some parameters/constants was needed. It included: (i) increase of forward and reverse rate parameters of SR Ca^{2+} pump (v_{maxf} and v_{maxr}) to $0.25\,\mathrm{mM\,s^{-1}}$ and

$0.75\,\mathrm{mM\,s^{-1}}$ respectively; (ii) decrease of on- and off-rate constants controlling adaptation of RyR channels (K_c^+ and K_c^-) to $0.1\,\mathrm{ms^{-1}}$ and $0.0008\,\mathrm{ms^{-1}}$ respectively; (iii) increase of the time constant controlling the diffusion of Ca^{2+} from NSR to JSR (τ_{tr}) to 20 ms; (iv) decrease of the time constant controlling the diffusion of Ca^{2+} from the dyadic space into the cytosol (τ_{xfer}) to 18 ms.

2.5. Numerical integration technique

The model was implemented in the program system MATLAB 6.5 (developed by the MathWorks, Inc.) and the numerical computation of the system of 121 non-linear differential equations was performed using the solver for stiff systems ODE-15s. The model was run for 10 minutes of equivalent cell lifetime to ensure that steady-state was reached. The values of all variables at this time were assigned as starting values before running model trials. The setting described in this section is referred to as basic adjustment of the model in the further text.

The basic units in which the equations were solved were: mV for membrane voltage, μA for membrane currents, mM for ionic concentrations, s for time, and mL for volumes. The adjustment of the model described in this section is referred to as basic in the further text.

3. Results

Fig. 2 illustrates action potentials (APs), three dominant membrane currents I_{Ca}, I_{Kto}, and I_{K1} and variations of Ca^{2+} and K^+ concentrations in different segments of tubular lumen at 1 Hz and 2.5 Hz steady state stimulation. While the differences between APs at surface and t-tubular membrane are minimal, the differences between surface and t-tubular components of membrane currents are marked. They are caused by uneven distribution of corresponding ion transporters between both membrane systems (see Tab. 1) but also partly by the changes of t-tubular ion concentrations during the stimulation cycle. The depletion of t-tubular Ca^{2+} is predominantly induced by activation of t-tubular I_{Ca} ($I_{Ca,t}$) and the two peaks in the t-tubular K^+ accumulation result from the activation of t-tubular I_{Kto} ($I_{Kto,t}$) in the beginning of AP and from the increase of t-tubular I_{K1} ($I_{K1,t}$) at AP repolarisation. The differences in the traces of $[Ca^{2+}]_t$ and of $[K^+]_t$ also indicate a presence of luminal ion concentration gradients in radial direction. The activity-induced depletion of t-tubular Ca^{2+} and accumulation of t-tubular K^+ peak in the vicinity of t-tubular membrane.

Fig. 3 shows the temporal relationship between the changes in $[Ca^{2+}]_{t1}$ and the intracellular Ca^{2+} transient during an action potential at steady-state 1 Hz and 2.5 Hz stimulation. To investigate whether the change of luminal $[Ca^{2+}]$ modulates Ca^{2+} flux across the t-tubule membrane and Ca^{2+} transient in the cytosol, the simulations were repeated while $[Ca^{2+}]$ in the t-tubule lumen was held constant at the concentration in the external bulk space (dotted lines). The differences between the results indicate that the decrease of luminal $[Ca^{2+}]$ has an effect on Ca^{2+} fluxes across the t-tubule membrane and thus on intracellular (cytosolic) Ca^{2+} transient. Quantification of this effect from the change of time integral (area) of Ca^{2+} transients showed their reduction by 2.5 % and 3.4 % at 1 Hz and 2.5 Hz, respectively.

Because of the paucity of experimental data related to human ventricular myocytes, the t-tubular fractions of ion transporters were preliminary set to be consistent with the model of guinea pig ventricular cells (Tab. 1, [3]). To explore the effect of Ca^{2+} concentration changes in t-tubules on cytosolic Ca^{2+} transient for potentially different combinations of

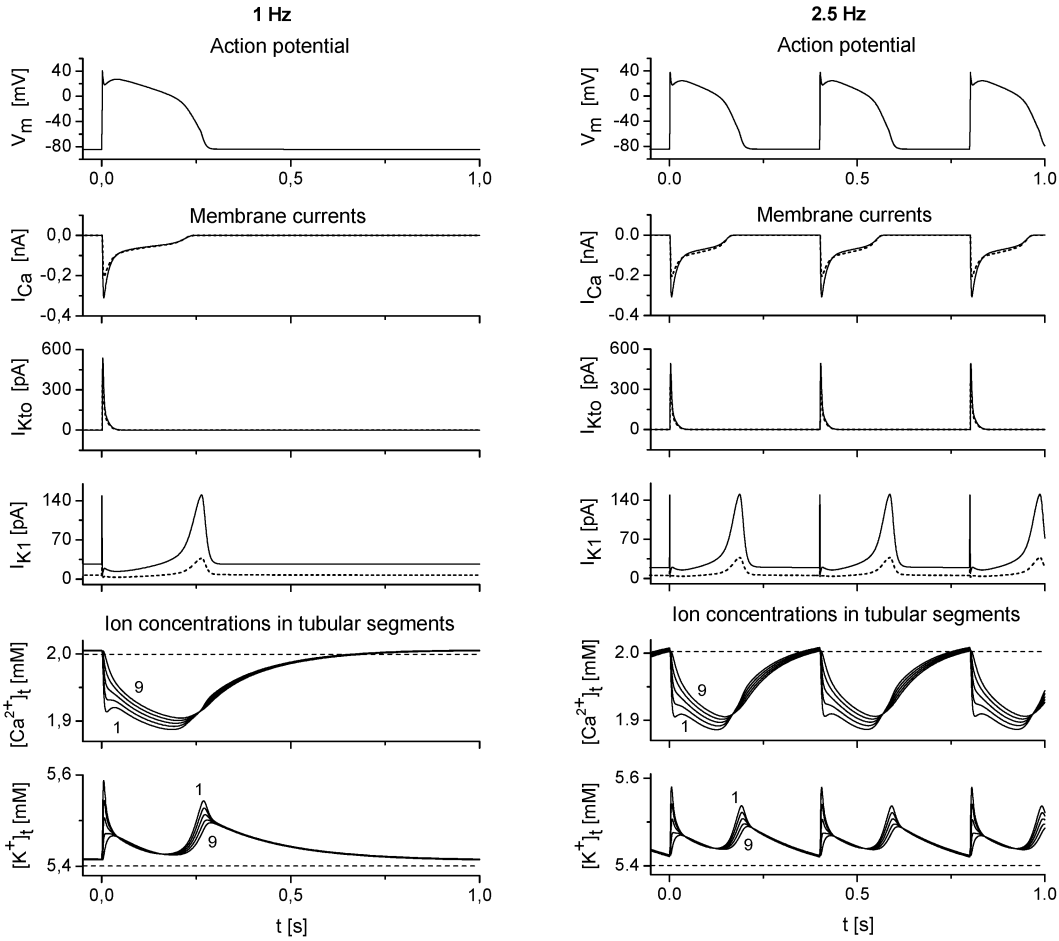

Fig.2: Action potentials (V_m), selected membrane currents (I_{Ca}, I_{Kto}, I_{K1}) and ion concentrations in the 1st, 3rd, 5th, 7th and 9th segment of tubular lumen ($[Ca^{2+}]_t$, $[K^+]_t$) at 1 Hz and 2.5 Hz steady-state stimulation. The continuous and dotted lines refer to t-tubular and surface membrane, respectively. Horizontal dashed lines show the levels of external ion concentrations ($[Ca^{2+}]_e = 2\,mM$ and $[K^+]_e = 5.4\,mM$).

fractions $f_{NaCa,t}$ and $f_{pCa,t}$ in human ventricular cells, we performed a series of simulations enabling to construct these relations in 3D-graphs (Fig. 4). The results showed that, if the fraction $f_{pCa,t}$ is small, the reduction of Ca^{2+} transient might be between 2 % and 3 % at resting heart rate (1 Hz) and between 3 % and 4 % during activity (2.5 Hz). However, high values of $f_{pCa,t}$ even led to accumulation of Ca^{2+} in the t-tubular space and consequently to a slight increase of Ca^{2+} transient.

The above described effect exhibited also a significant dependence on the rate of Ca^{2+} exchange between external space and t-tubules as illustrated in Fig. 5. In the model with basic adjustment, increase of $\tau_{Ca,extt}$ from the basic value of 240 ms to 480 ms and 960 ms resulted in reduction of Ca^{2+} transient respectively by 3.8 % and 6.1 % at 1 Hz stimulation and by 5.3 % and 9.9 % at 2.5 Hz stimulation.

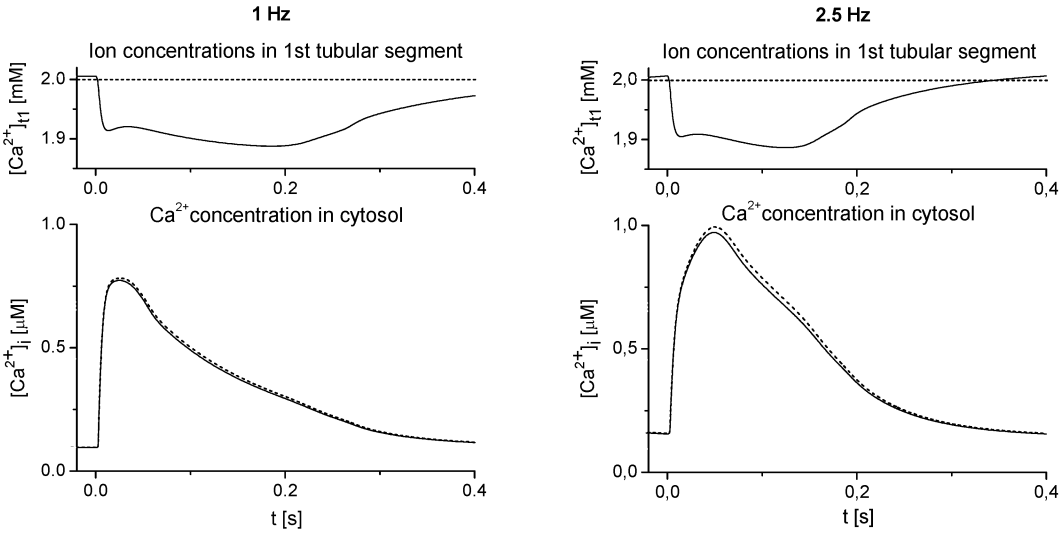

Fig.3: Effect of Ca^{2+} concentration changes in the first t-tubular segment ($[Ca^{2+}]_{t1}$) on Ca^{2+} transient in the cytosol ($[Ca^{2+}]_i$) during a steady state stimulation at 1 Hz and 2.5 Hz. The model was run when t-tubular ion concentrations were either allowed to change (black lines) or fixed at external levels (dotted lines).

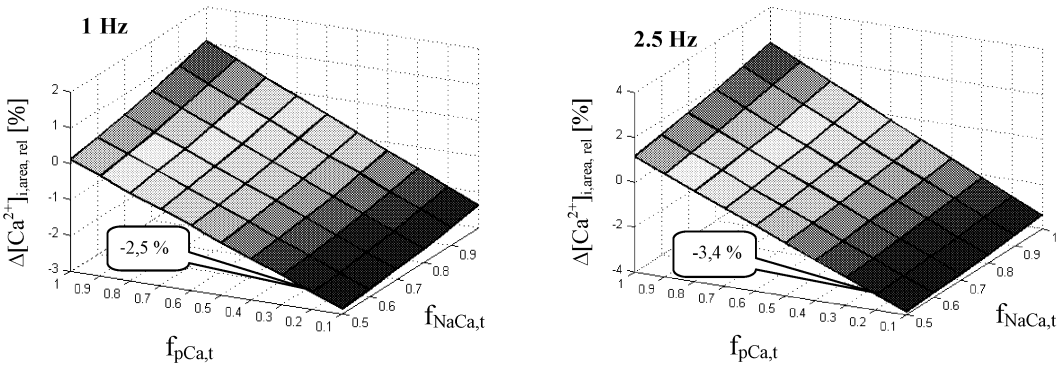

Fig.4: Effect of values of $f_{\mathrm{pCa,t}}$ and $f_{\mathrm{NaCa,t}}$ on intracellular Ca^{2+} transient during a steady state cycle at 1 Hz and 2.5 Hz. The values in rectangle indicate the percentage reduction of the cytosolic Ca^{2+} transient for basic adjustment of $f_{\mathrm{NaCa,t}}$ (0.56) and $f_{\mathrm{pCa,t}}$ (0.2) specified in Tab. 1. $\Delta[Ca^{2+}]_{\mathrm{i,area,rel}}$ represents percentage change of the area of cytosolic Ca^{2+} transient during a whole cycle relative to the area of steady state Ca^{2+} transient in the model with tubular ion concentrations fixed at external levels.

4. Discussion and Conclusions

Quantitative models based on the specific properties of human cardiac cells are desirable from the point of view of experimental and clinical cardiology. The availability of the needed data is, however, strongly limited due to inaccessibility of biological material. Therefore, human models are generally based on animal models, into which the data obtained from human cardiomyocytes left after surgery are gradually incorporated. The present model of

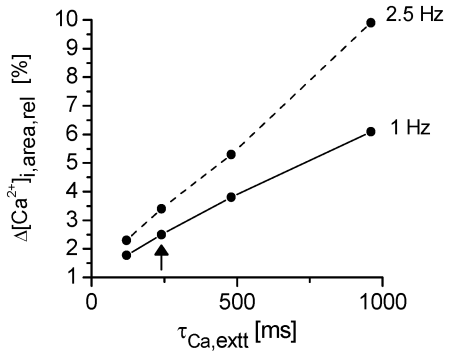

Fig.5: Effect of time constant controlling exchange of Ca^{2+} between external and tubular space ($\tau_{Ca,extt}$) on the percentage reduction of the cytosolic Ca^{2+} transient ($\Delta[Ca^{2+}]_{i,area,rel}$). $\Delta[Ca^{2+}]_{i,area,rel}$ represents percentage change of the area of cytosolic Ca^{2+} transient during a whole cycle relative to the area of steady state Ca^{2+} transient in the model with tubular ion concentrations fixed at external levels. Solid and dashed lines refer to simulated steady state values at 1 and 2.5 Hz, respectively. The arrow denotes the basic setting of $\tau_{Ca,extt}$ in the model.

ventricular cell comprises a number of data from experiments on isolated human cardiac cells related to morphology of t-tubules, and to the particular properties of ion transfer mechanisms.

To increase the accuracy, the present model was upgraded by incorporation of a description of ion diffusion within t-tubular lumen in radial direction. The simulations suggest that, depending on the underlying parameters, the activity-induced variations of Ca^{2+} concentration in human t-tubules might lower Ca^{2+} entry into the cell and thus reduce the intracellular Ca^{2+} transients that control the strength of cellular contraction. The effect would be significant provided the values of the parameters (unknown for human cardiac cells up to date) satisfied the following conditions: (i) high fraction of Ca^{2+} channels in t-tubular membrane ($f_{Ca,t} > 0.64$); (ii) low fraction of active Ca^{2+}-transporting proteins ($f_{pCa,t} < 0.2$); (iii) slow rate of Ca^{2+} exchange between extracellular spaces and t-tubular lumen ($\tau_{Ca,extt} > 240$ ms).

The definite answer to the question of the effect of concentration changes in human t-tubules on calcium turnover can be given in the future provided new data about localization of ion transporters in the t-tubule membrane and rate of ion diffusion between t-tubular lumen and extracellular spaces in human hearts are available.

Acknowledgment

This study was realised with institutional support RVO:61388998, with support of the university project MUNI/A/0951/2012, and a support by Université Lyon 1 research allowances to the EA4612 Neurocardiology Unit.

Appendix

Abbreviations used in the text

Symbol	Definition
AP	Action potential
SR	Sarcoplasmic reticulum
NSR	Network compartment of SR
JSR	Junctional compartment of SR
RyR	Ryanodine receptor

Variables used in the text

Symbol	Definition
V_{m}	Membrane voltage
I_{Na}	Fast Na^+ current
I_{Ca}	L-type Ca^{2+} current
I_{Naps}	Persistent Na^+ current
I_{Kto}	Transient outward K^+ current
I_{Kp}	Plateau K^+ current
I_{Kr}	Rapid delayed rectifier K^+ current
I_{Ks}	Slow delayed rectifier K^+ current
I_{K1}	Inward rectifying K^+ current
$I_{\mathrm{K(Na)}}$	Sodium-activated K^+ current
$I_{\mathrm{K(ATP)}}$	ATP sensitive K^+ current
$I_{\mathrm{ns(Ca)}}$	Calcium-activated nonspecific current
I_{b}	Background current
I_{NaCa}	Na^+ – Ca^{2+} exchange current
I_{NaK}	Na^+ – K^+ pump current
I_{pCa}	Ca^{2+} pump current
$I_{\mathrm{i,s}}$	Surface membrane component of current i
$I_{\mathrm{i,t}}$	Tubular membrane component of current i
J_{up}	Ca^{2+} flow via SR Ca^{2+} pump
$[\mathrm{x}]_{\mathrm{e}}$	Free concentration of substance x in external space
$[\mathrm{x}]_{\mathrm{t}}$	Free concentration of substance x in t-tubular space
$[\mathrm{x}]_{\mathrm{d}}$	Free concentration of substance x in dyadic space
$[\mathrm{x}]_{\mathrm{i}}$	Free concentration of substance x in cytosol
$[\mathrm{x}]_{\mathrm{JSR}}$	Free concentration of substance x in JSR
$[\mathrm{x}]_{\mathrm{NSR}}$	Free concentration of substance x in NSR

Parameters/constants used in the text

Symbol	Definition
V_{cell}	Total volume of cell
A_{tot}	Total membrane area
A_{surf}	Area of surface membrane
A_{tub}	Area of t-tubular membrane
$f_{\mathrm{i,t}}$	Fraction of ion transporters i in t-tubular membrane
$\tau_{\mathrm{x,extt}}$	Time constant of ion x exchange between external space and t-tubules

References

[1] Ohlídalová D., Pásek M., Šimurda J., Christé G.: Physiological consequences of ion concentration changes in transverse-axial tubular system in a model of human ventricular cardiomyocyte, In: Proc. 20th Bienni. Int. Conf. Biosignal, Brno 2010, p. 114–117

[2] Pásek M., Christé G., Šimurda J.: The functional role of cardiac t-tubules in a model of rat ventricular myocytes, Phil. Trans. R. Soc. A. 364 (2006) 1187–1206

[3] Pásek M., Christé G., Šimurda J.: A model of the guinea-pig ventricular cardiac myocyte incorporating a transverse-axial tubular system, Prog. Biophys. Mol. Biol. 96 (2008) 258–280

[4] Ohler A., Weisser-Thomas J., Piacentino V. 3rd, Houser S.R., Tomaselli G.F., O'Rourke B.: Two-Photon Laser Scanning Microscopy of the Transverse-Axial Tubule System in Ventricular Cardiomyocytes from Failing and Non-Failing Human Hearts, Cardiol. Res. Pract. 2009 (2009) 1–9

[5] Iyer V., Mazhari R., Winslow R. L.: A computational model of the human left-ventricular epicardial myocyte, Biophys. J. 87 (2004) 1507–1525

[6] Ten Tusscher K.H.W.J., Noble D., Noble P.J., Panfilov A.V.: A model for human ventricular tissue, Am. J. Physiol. 286 (2004) 1573–1589

[7] Li G.R., Feng J., Yue L., Carrier M.: Transmural heterogeneity of action potentials and Ito1 in myocytes isolated from the human right ventricle, Am. J. Physiol. 275 (1998) 369–377

[8] Beuckelmann D.J., Näbauer M., Erdmann E.: Intracellular calcium handling in isolated ventricular myocytes from patients with terminal heart failure, Circulation 88 (1992) 1046–1055

[9] Pieske B., Houser S.R.: $[Na^+]_i$ handling in the failing human heart, Cardiovasc. Res. 57 (2003) 874–886

Received in editor's office: March 22, 2013
Approved for publishing: June 21, 2013